JOURNAL OF GEOPHYSICAL RESEARCH, VOL. 103, NO. C4, PAGES 7537–7548, APRIL 15, 1998

On the western boundary currents in the Philippine Sea

Tangdong Qu

Japan Marine Science and Technology Center, Yokosuka
Institute of Oceanology, Chinese Academy of Sciences, Qingdao, China

Humio Mitsudera[1]

Japan Marine Science and Technology Center, Yokosuka

Toshio Yamagata

Department of Earth and Planetary Physics, Tokyo University, Tokyo

Abstract. In this study we describe the velocity structure and transport of the North Equatorial Current (NEC), the Kuroshio, and the Mindanao Current (MC) using repeated hydrographic sections near the Philippine coast. A most striking feature of the current system in the region is the undercurrent structure below the surface flow. Both the Luzon Undercurrent and the Mindanao Undercurrent appear to be permanent phenomena. The present data set also provides an estimate of the mean circulation diagram (relative to 1500 dbar) that involves a NEC transport of 41 Sverdrups (Sv), a Kuroshio transport of 14 Sv, and a MC transport of 27 Sv, inducing a mass balance better than 1 Sv within the region enclosed by stations. The circulation diagram is insensitive to vertical displacements of the reference level within the depth range between 1500 and 2500 dbar. Transport fluctuations are, in general, consistent with earlier observations; that is, the NEC and the Kuroshio vary in the same phase with a seasonal signal superimposed with interannual variations, and the transport of the MC is dominated by a quasi-biennial oscillation. Dynamic height distributions are also examined to explore the dynamics of the current system.

1. Introduction

The North Equatorial Current (NEC) in the Pacific bifurcates as it approaches the Philippine coast, feeding the northward flowing Kuroshio and the southward flowing Mindanao Current (MC). The NEC-Kuroshio-MC current system is important because of its role in the heat budget of the western Pacific warm pool [*Qu et al.*, 1997a] and its direct involvement in the global ocean thermohaline circulation via the Indonesian throughflow [*Gordon*, 1986], both of which are believed to be essential in determining the world's climate [*Lukas et al.*, 1996]. Also, the current system is part of the shallow, meridional, wind- and buoyancy-flux-driven circulation that directly connects the subtropical and equatorial oceans [*McCreary and Lu*, 1994]. Studies of the current system have significantly advanced our knowledge of its mass and heat transport, in particular with regard to its variabilities. By comparing the time series of subsurface temperature in the Kuroshio extension with that of the NEC transport, *Yamagata et al.* [1985] found a significant correlation between the interannual changes of the two currents, suggesting that the interannual variability of the Kuroshio extension primarily follows the El Niño–Southern Oscillation (ENSO) with a time lag of about 1.5 years. *Lukas* [1988], using the daily sea level at Davao and Malakal, inferred that the MC transport is dominated by interannual variations, in which an intermittent quasi-biennial signal is more prominent than the ENSO signal. Baroclinic signature with large-amplitude variabilities was also observed in the current system [e.g., *Wyrtki*, 1961; *Nitani*, 1972; *Toole et al.*, 1990; *Hu et al.*, 1991; *Lukas et al.*, 1991; *Qu et al.*, 1997b]. Among others, *Hu et al.* [1991] revealed the existence of the Mindanao Undercurrent (MUC) flowing northward below and offshore of the MC, and *Qu et al.* [1997b] found the Luzon Undercurrent (LUC) flowing southward on the inshore edge of the Kuroshio.

A reliable picture of the mean flow in the NEC-Kuroshio-MC system was not provided by the earlier studies, mainly because measurements with temporally repeated and spatially extensive coverage were not used. Also, owing to the scarcity of direct measurements, most of the previous studies were based on the assumption of geostrophy. Geostrophic estimates of velocity from individual hydrographic sections may introduce substantial noise [*Lukas et al.*, 1991], primarily due to strong eddies and internal tides in the region [*Masumoto and Yamagata*, 1991; *Qiu and Lukas*, 1996]. To enhance the signal-to-noise ratio, repeated sections are highly desirable.

On the basis of eight hydrographic sections along 8°N in the western Pacific, *Wijffels et al.* [1995] recently presented an interesting study in which they described the mean structure and transport of the MC. In the upper layer waters they compared the averaged geostrophic currents with directly measured velocity sections using an acoustic Doppler current profiler (ADCP) and found them to be identical to within the estimated errors. This warranted more detailed analysis with time-averaged hydrographic data. The mean structure of the Kuroshio and its underlying LUC were explored more recently

[1]Now at International Pacific Research Center, University of Hawaii, Honolulu.

Copyright 1998 by the American Geophysical Union.

Paper number 98JC00263.
0148-0227/98/98JC-00263$09.00

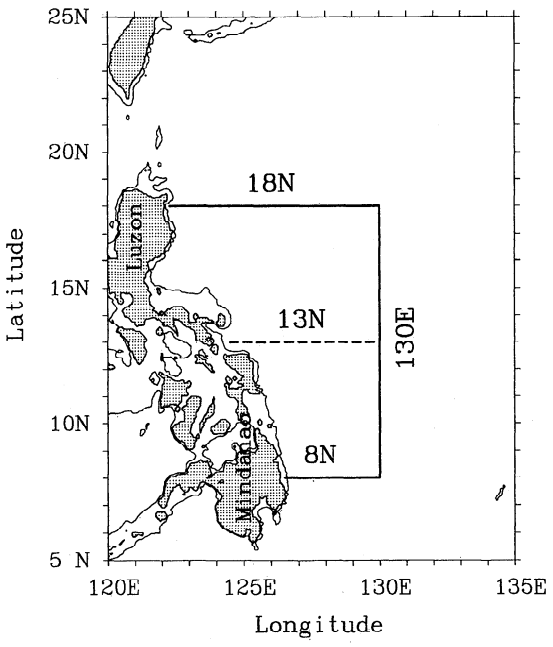

Figure 1. Map of the Philippine Sea showing the location of repeated hydrographic sections. The thin lines represent the 500-m isobath.

by *Qu et al.* [1997b] using a repeated hydrographic section east of Luzon. Although these two studies have shown many important features of the MC and the Kuroshio, they did not consider the currents as a whole system. A comprehensive description of the NEC-Kuroshio-MC current system is still lacking.

Fourteen oceanographic surveys were conducted in the tropical western Pacific from 1986 through 1991 under the auspices of Tropical Ocean and Global Atmosphere (TOGA) and World Ocean Circulation Experiment (WOCE): five by the Chinese Academy of Sciences (CAS) and nine by a cooperative program between the People's Republic of China and the United States (PRC-US). During these surveys the NEC was sampled at 130°E, the Kuroshio was sampled at 18°N, and the MC was sampled at 8°N (Figure 1). The repeated hydrographic sections likely provide the most reliable picture to date of the current structure and transport in the NEC-Kuroshio-MC system near the Philippine coast.

2. Data and Method

The CAS surveys occurred every September–October from 1986 through 1990, taking hydrographic (conductivity-temperature-depth (CTD)) measurements along 130°E, 18°N, and 7°30′N, except for CAS 1, during which the NEC and the MC were sampled at different sections. To explore the bifurcation dynamics of the NEC, CTD casts were also made at 13°N (dashed line in Figure 1) during three CAS cruises (CAS 1, 3, and 4) in 1986, 1988, and 1989, respectively. The PRC-US surveys were distributed over almost all seasons of the year during the time period 1986–1991, with one (PRC-US 1) in January–February, two (PRC-US 4 and 6) in April, one (PRC-US 8) in June, three (PRC-US 3, 5, and 7) in September–October, and two (PRC-US 2 and 9) in November, providing hydrographic crossings of the NEC at 130°E, of the Kuroshio at 18°20′N, and of the MC at 8°N. Cruises 1, 2, and 7 of this program made no observation along 8°N, and cruise 7 collected only two casts at 130°E. Most of the samples taken by the CAS program were extended to 1500 dbar, while those made by the PRC-US program reached at least 3000 dbar or to within 100 m of the ocean floor.

All the hydrographic casts used for the present study are shown in Figures 2a–2d, where the minor latitudinal differences between the CAS and the PRC-US cruises are disregarded in two zonal sections. Altogether, the hydrographic sections were repeated 12 times at 130°E, 14 times at 18°N, 10 times at 8°N, and 3 times at 13°N, with more than half of them taking place in the boreal fall. Our attention below will be focused primarily on three boundary sections (solid lines in Figure 1). The relatively less sampled section at 13°N is to be used mainly for exploring the dynamics associated with the NEC bifurcation.

The mean hydrographic sections were constructed by averaging in 0.5°-longitude bins at 18° and 8°N and in 1°-latitude bins at 130°E. The number of samples in each bin is usually >10 and can be as large as 40 near the western boundary. The number of samples near the western boundary decreases with depth, owing to the presence of the continental shelf, to ~20 at 1500 dbar and ~5 at 3000 dbar. To limit the artificial smoothing of features in the vertical obtained when averaging on pressure surfaces around the pycnocline, we performed the averaging first on a set of potential density surfaces with a 0.02 kg m^{-3} vertical resolution. Close to the surface, the concept of averaging on potential density surfaces breaks down because of the occasional outcropping of isopycnals. Following *Gouriou and Toole* [1993], the average properties between the mean mixed layer base (defined as the first depth at which the potential density is 0.1 kg m^{-3} greater than the surface value) and the first isopycnal surface present on all cruises were obtained by linear interpolation. Then the average properties were interpolated back to a 10-dbar uniform pressure series.

3. Background From Climatology

Geostrophic flow fields are shown at 100, 300, and 500 dbar from *Levitus*' [1982] annual mean temperature and salinity climatology by assuming a 1500 dbar reference level (Figures 3a–3c). As the objective analysis used in preparing this data set involves smoothing over 1000 km, the smoothed fields may not be appropriate for showing the detailed phenomena associated with the narrow western boundary currents. Nevertheless, the historical data provide a basic background for further investigating the current system in the region.

The broad westward directed NEC can be seen with different intensity and location at three different depths. Near the surface (Figure 3a) the NEC is located primarily between 8° and 16°N, achieving speeds of the order of 0.2 m s^{-1} at 13°–14°N. As it progresses to the deeper levels, this westward flow becomes weaker and shifts to the north (Figures 3b and 3c). The bifurcation of the NEC, defined to be where the meridional velocity averaged within the 2°-longitude band from the coast is zero, consequently, moves from ~13.5°N at the surface to ~18°N at 500 dbar (Figure 3d). On the vertical average (0–500 m) the bifurcation of the NEC occurs at ~15°N.

The northward shift of the NEC and its bifurcation could be explained in two ways: either as a result of interaction between the Sverdrup transport and the boundary constraints on density [*Reid and Arthur*, 1975] or as a result of counterbalance between the layer thickness change and the meridional plane-

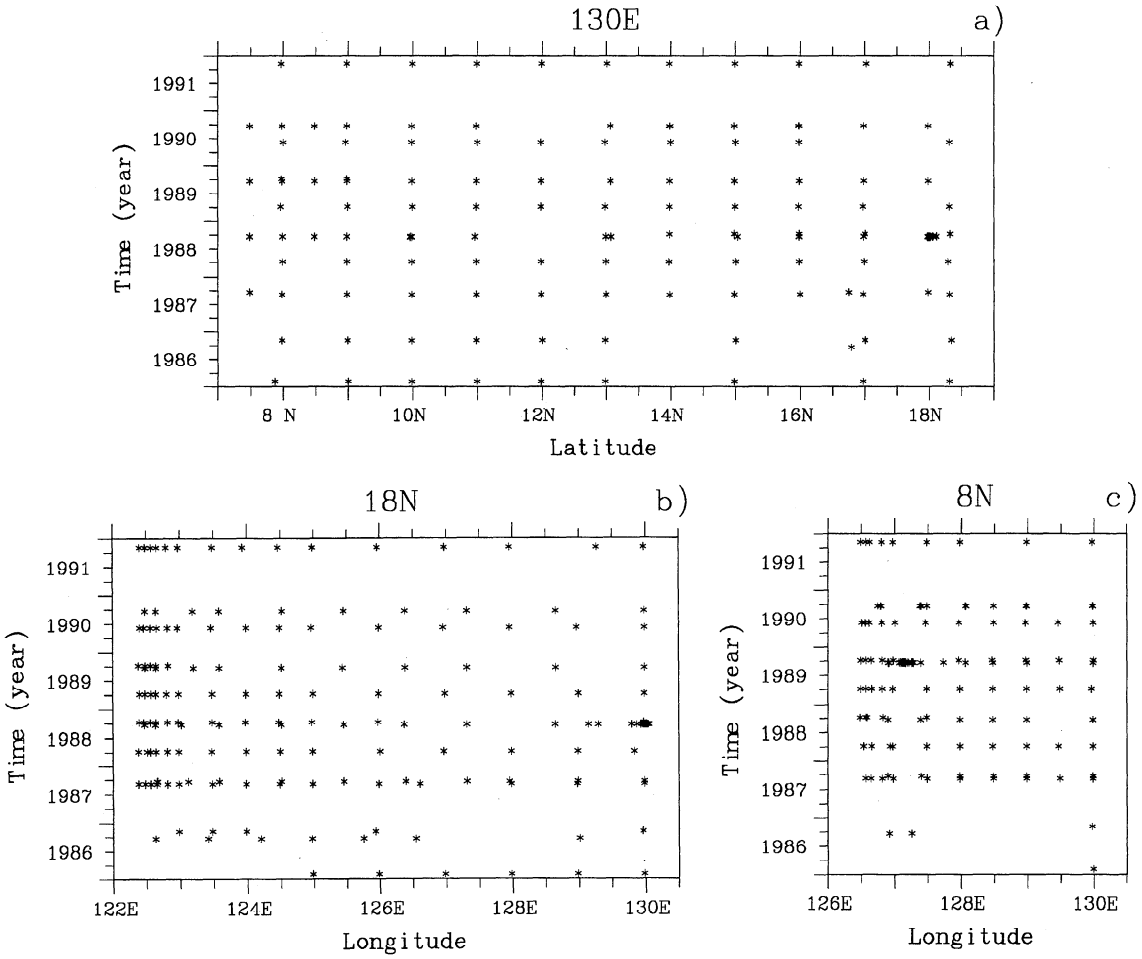

Figure 2. Spatial and temporal distribution of hydrographic stations (asterisk) at (a) 130°E, (b) 18°N, (c) 8°N, and (d) 13°N.

tary vorticity variation across the current [*Toole et al.*, 1990]. In the subtropical gyre, of which the NEC is the southern component, Ekman transport is generally convergent, producing a downward movement and thus a high-pressure ridge around the center of the gyre, with isobars sloping down toward either side. In response, water below the Ekman layer moves, geostrophically, westward (NEC) in the southern part of the gyre, with an equatorward component in order that the geostrophic divergence can gradually counterbalance the Ekman convergence. In the meantime, water density tends to increase poleward near the surface because of the latitude-dependent surface heat flux. This density change near the surface causes a reduction in the slope of the southern portion of upper isobars and, consequently, an equatorward shift of the high-pressure ridge: the northern boundary of the NEC, as we approach the surface [see *Reid and Arthur*, 1975]. In an independent way, *Toole et al.* [1990] found nearly constant potential vorticity within the NEC. As relative vorticity is small in the ocean interior compared to f (<10% in their case), potential vorticity is largely determined by the quantity f/h, where f represents the Coriolis frequency or the planetary vorticity and h is the thickness of the current. To keep f/h constant, the latitudinal variation of the Coriolis frequency must be compensated by the change in the thickness of the current, thus making the NEC spread to deeper waters as we progress to the north.

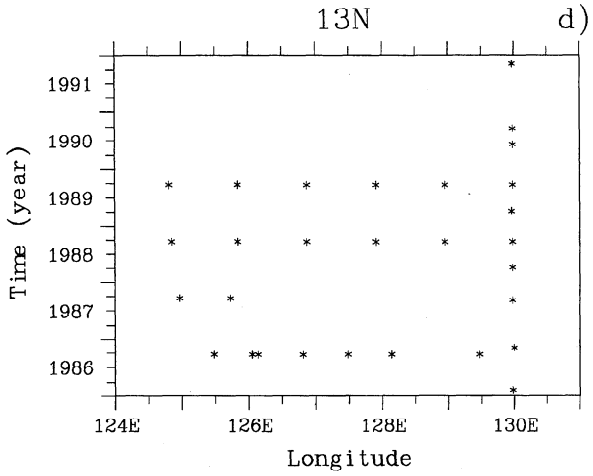

Figure 2. (continued)

4. Current Structure and Transport

4.1. Mean Structure

An initial level of no motion for geostrophic calculation of mean velocity is chosen at 1500 dbar, the deepest common depth of the observations. Figure 4a illustrates the zonal flow

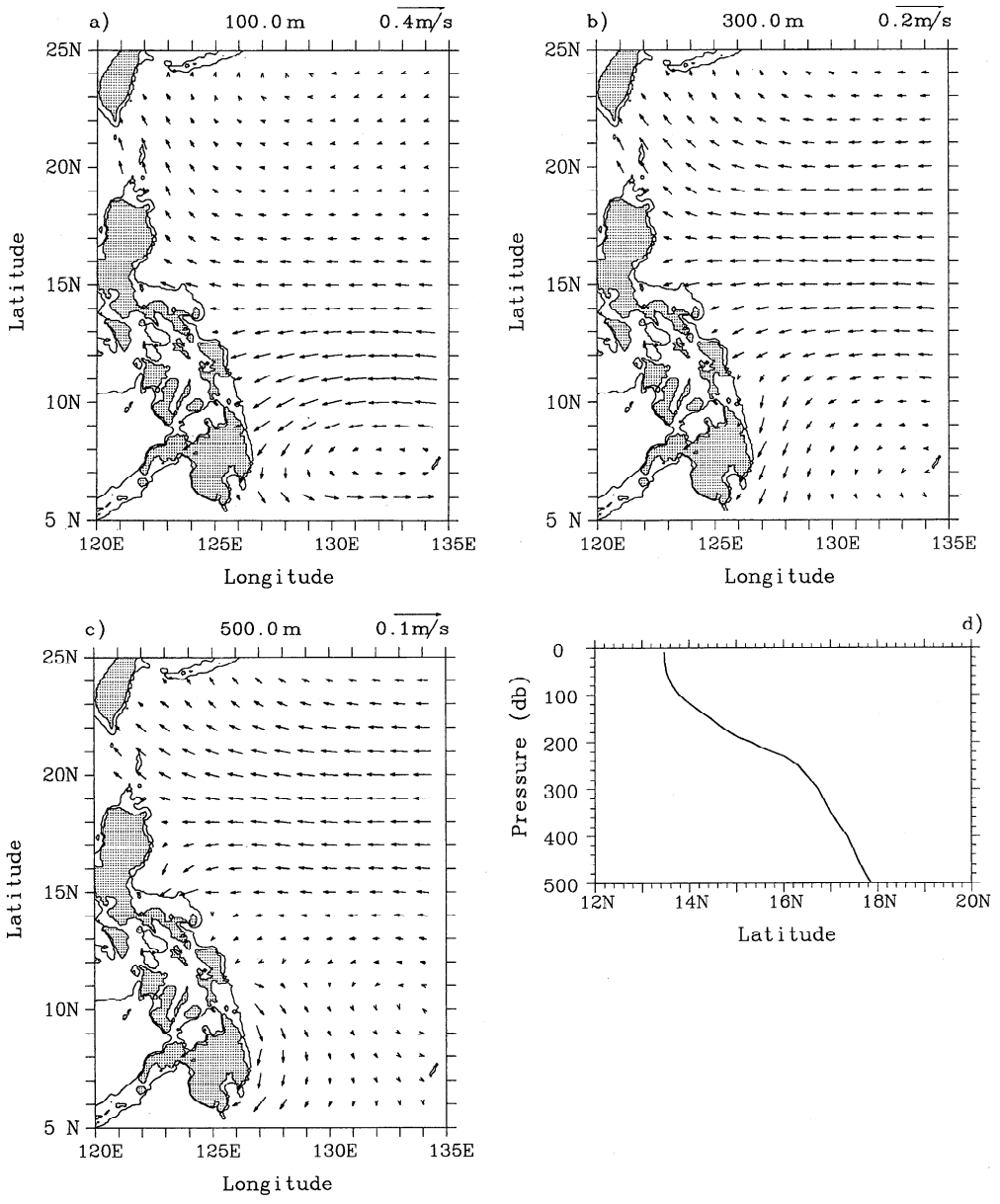

Figure 3. Geostrophic velocity field relative to 1500 dbar from *Levitus'* [1982] annual mean temperature and salinity climatology at (a) 100, (b) 300, and (c) 500 m and (d) vertical profile of the North Equatorial Current (NEC) bifurcation latitude.

derived from mean temperature and salinity sections at 130°E. The NEC is seen throughout the section, contracting poleward on denser waters from ~300 m at 8°N to ~800 m at 18°N. The velocity of the NEC exceeds 0.2 m s^{-1} in a broad area between 9° and 13°N, having two maxima at 9.5° and 12.5°N, respectively. The high-speed core at 12.5°N is consonant with the flow field of climatology (Figure 3a), while the relatively high speeds around the southern end are likely to be related to the Mindanao Eddy located at about 130°E and 7°N [*Wyrtki*, 1961; *Lukas et al.*, 1991]. Below the NEC, weak eastward flow is indicated with maximum velocity exceeding 0.05 m s^{-1} at ~10.5°N.

The Kuroshio is confined within the upper 500 m and ~200 km from the Philippines, with its baroclinic velocity exceeding 0.45 m s^{-1} near the surface (Figure 4b). The alternating bands of the northward and southward flows east of the Kuroshio could be due to the warm eddy observed east of the Luzon Strait [*Nitani*, 1972; *Guan*, 1983]. The subsurface countercurrent below the Kuroshio has been reported and called the Luzon Undercurrent (LUC) by *Qu et al.* [1997b]. Using the same hydrographic data, they noted that the LUC is located on the shelf slope with its upper and lower boundaries at ~500 and 2000 m, respectively. While its absolute velocity may depend on the choice of reference level, for example, with a maximum value of ~0.07 m s^{-1} relative to 2500 dbar and ~0.04 m s^{-1} relative to 1500 dbar, the basic structure of the LUC seems to be robust.

The MC becomes well developed at 8°N. It is separated by a weak northward flow into two parts (Figure 4c). The inshore part is about 200 km wide and has an intense velocity core over 0.8 m s^{-1} near the surface. It narrows with depth to a width of ~100 km at 500 m. The offshore part is relatively weak. This upper layer pattern closely resembles the direct ADCP measurements described by *Wijffels et al.* [1995, Figure 5b].

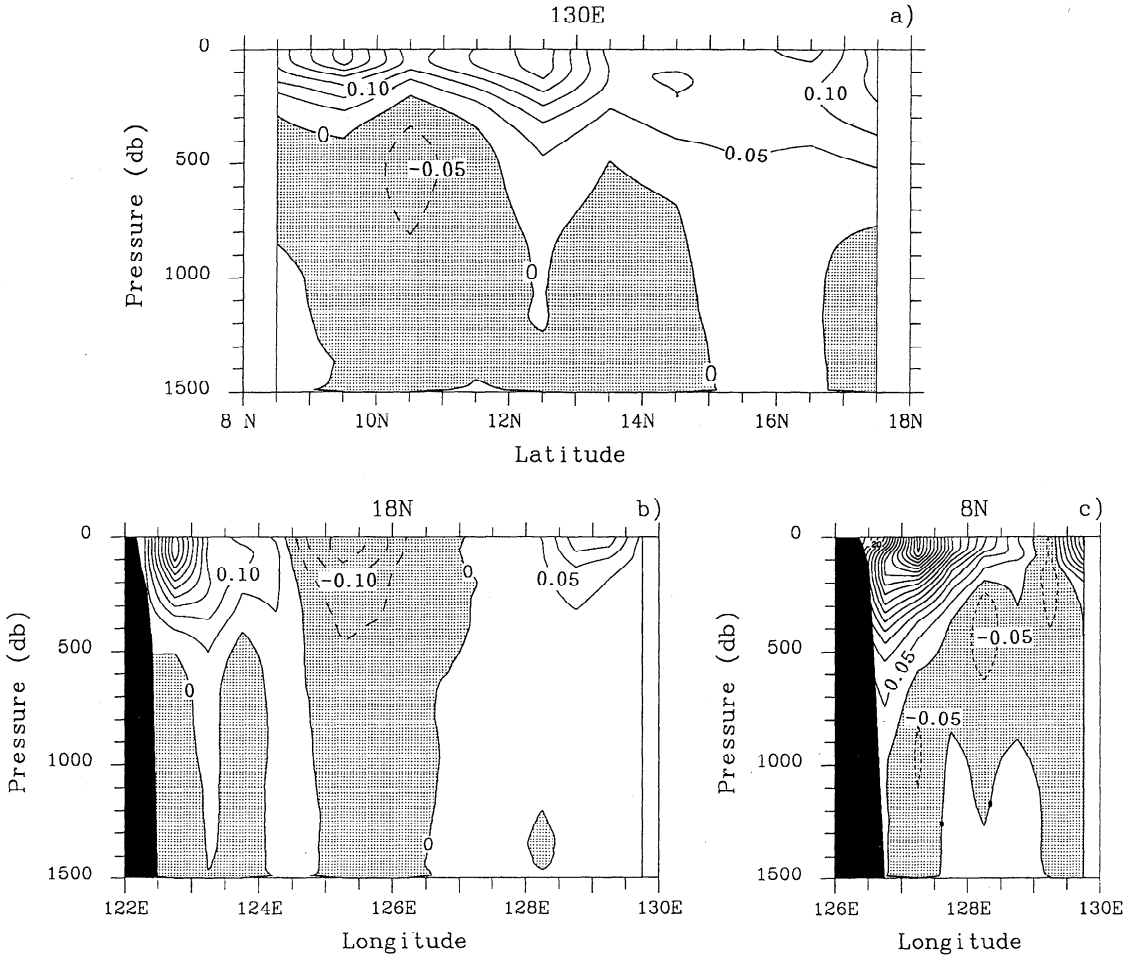

Figure 4. Geostrophic mean velocities (m s^{-1}) derived from mean hydrographic sections (relative to 1500 dbar) at (a) 130°E, (b) 18°N, and (c) 8°N. The contour intervals are 0.05 m s^{-1}, and positive values are westward for the NEC, northward for the Kuroshio, and southward for the Mindanao Current (MC).

The undercurrent structure below the MC has previously been reported by several studies. On three cruises (CAS 2, 3, and 4) along 7.5°N, *Hu et al.* [1991] observed multiple subsurface northward velocity cores (the MUC) off Mindanao with speeds of 0.15–0.30 m s^{-1}. This picture was confirmed by a snapshot ADCP measurement during the Western Equatorial Pacific Ocean Circulation Study (WEPOCS-III), and the MUC was found to be 20–25 km wide and 50–75 km offshore [*Lukas et al.*, 1991]. Here the mean section (Figure 4c) shows two northward velocity cores at 900 dbar, 127.25°E and at 400 dbar, 128.5°E, respectively.

Using seven directly measured velocity sections, *Wijffels et al.* [1995, Figure 5b] noted weak mean northward flow below and offshore of the MC, which led them to the conclusion that the MUC is just a transient phenomenon. Consonant with their conclusion, the shallower northward velocity core in Figure 4c seems to be more sensitive to the choice of the reference level, becoming weaker with increasing depth of no motion (discussed in section 4.3). However, *Wijffels et al.* [1995] did not show the velocity field below 400 dbar, so their conclusion is not likely to fit the deeper waters. In fact, a northward flow might be identified in their mean potential density section [*Wijffels*, 1995, Figure 3a] by the downward slope of isopycnals from ~500 down to 1000 dbar offshore of the MC. Furthermore, the lower part of the northward flow, occurring between 27.1 and 27.4 σ_θ surfaces, coincides basically with the elevated (>2.0 mL L^{-1}) oxygen concentrations [*Wijffels et al.*, 1995, Figure 4b]. Such an oxygen rich subsurface water is unambiguously of southern hemisphere origin [*Fine et al.*, 1994]. These results seem to mean that the MUC, referred to as the deeper northward velocity core, should be a permanent feature.

4.2. Mean Transport

Mean transports in the upper 1500 dbar (Table 1) were estimated by assuming several reference levels ranging from 1500 to 2500 dbar, where velocities west of the first station pair in zonal sections were extrapolated to zero at the coast. To show the relative components of water masses, transport estimates were also subdivided into an upper thermocline layer ($\sigma_\theta < 26.7$), a lower thermocline layer ($26.7 < \sigma_\theta < 27.1$), and an intermediate layer ($27.1\sigma_\theta$-1500 dbar). In the upper thermocline a westward transport of about 45 Sv (1 Sv = 10^6 m^3 s^{-1}) is computed for the NEC, a northward transport of about 13 Sv is computed for the Kuroshio, and a southward transport of 27–28 Sv is computed for the MC. These values are partially offset by the countercurrents in the lower thermocline and intermediate layers, that is, the eastward flow below the NEC, the LUC, and the MUC. Total (0–1500) transports of the NEC-Kuroshio-MC system achieve a mass balance better than

Table 1. Geostrophic Transport in the Upper 1500 dbar Derived From Mean Hydrographic Sections at 130°E, 18°N, and 8°N

Depth of No Motion, dbar	$\sigma_\theta < 26.7$			$26.7 < \sigma_\theta < 27.1$			27.1 σ_θ-1500 dbar			0–1500 dbar		
	NEC	KC	MC	NEC	KC	MC	NEC	KC	MC	NEC	KC	MC
1500	45.1	13.4	27.7	0.5	0.2	0.9	−4.2	−0.2	−1.6	41.3	13.5	27.3
2000	44.8	12.4	27.8	0.2	−0.2	2.0	−4.2	−1.7	−1.2	41.0	10.6	27.9
2500	44.9	12.8	27.6	0.3	−0.1	1.0	−4.0	−1.1	−1.5	41.4	11.7	27.4

Geostrophic transport is in Sverdrups. Positive values are westward for the North Equatorial Current (NEC), northward for the Kuroshio Current (KC), and southward for the Mindanao Current (MC).

2 Sv in the upper 1500 dbar for all reference levels between 1500 and 2500 dbar.

The present results (Table 1) are compared with the mean circulation diagram of transport derived from the historical data [*Toole et al.*, 1988]. By assuming a 1000 dbar depth of no motion, *Toole et al.* [1988, Figure 3] reported a NEC transport of 45 Sv, a Kuroshio transport of 15 Sv, and a MC transport of 17 Sv above the 12°C isotherm. Their estimates were, in general, consistent with Table 1, except that the MC transport was underestimated by ~10 Sv, presumably because the spatial resolution (1°) employed in their analysis did not fully resolve the flow field adjacent to the MC as was expected. The underestimate of the MC transport certainly induced a residual of mass. To achieve mass balance, they apportioned the residual of mass to the two coastal flows on the basis of a surface NEC bifurcation latitude of 12°N; that is, Kuroshio transport equals NEC transport north of 12°N and the MC equals NEC transport south of 12°N, resulting in final estimates of 25 Sv for the Kuroshio and 18 Sv for the MC. We have reason to believe that such an apportionment [also *Toole et al.*, 1990] is not appropriate. The reason lies in the fact that the NEC bifurcation shifts northward with increasing depth. This means that the total meridional transport does not have to be zero at the surface NEC bifurcation latitude. With a repeated hydrographic section at 13°N a southward transport of >10 Sv was indeed found around the surface bifurcation of the NEC.

One of the important results inferred from *Toole et al.*'s [1988] mean circulation diagram is that the Indonesian throughflow is only of the order of 1 Sv. The value could be underestimated as a result of small MC transport. If their estimates of the South Equatorial Current (16 Sv) and the North Equatorial Countercurrent (33 Sv) still remain [*Toole et al.*, 1988, Figure 3], the present results suggest a throughflow transport of the order of 10 Sv, which seems to be more reasonable compared with recent observations [e.g., *Meyers et al.*, 1995].

4.3. The Depth of No Motion

Two minima of vertical shear are indicated in the mean potential density profiles (Figure 5). One is located around 2000 dbar, with slight differences at different sections, and the second is seen at ~4000 db, in consistency with the previous observations by *Toole et al.* [1990]. The vertical shear is relatively small within a broad depth range centered at 2000 dbar, so both velocity and transport are insensitive to ±500-dbar vertical displacements of the reference level around this depth. For the present data, of which many stations did not extend to 4000 dbar, 2000 dbar is likely to be the best choice for the reference level. Velocities relative to 2000 dbar are computed at two zonal sections (Figures 6a and 6b), in which the LUC and the MUC are found to exceed 0.05 and 0.08 m s^{-1} at ~700 and 900 dbar, respectively.

4.4. Variability

Geostrophic velocities relative to 1500 dbar are also calculated for individual cruises. Averaging of individual velocity sections provides independent information on the mean flow (not shown), which resembles Figures 4a–4c in all the details. Variability in geostrophic velocity is fairly large in the region, giving us an impression that the mean geostrophic flow is significant against its variability only at the high-speed core of

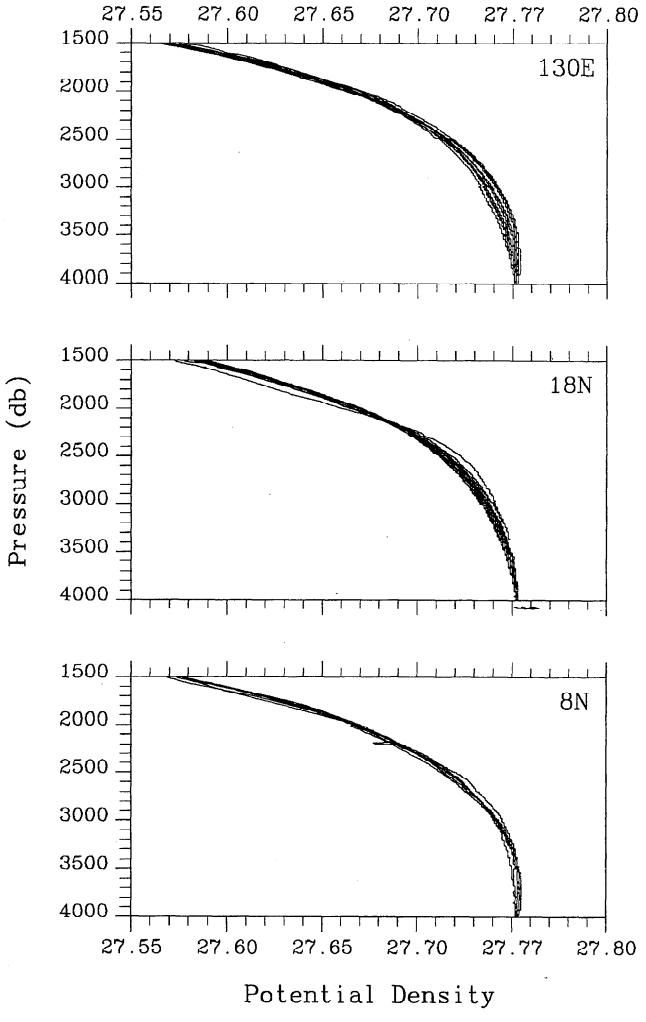

Figure 5. Vertical profiles of mean potential density at 130°E, 18°N, and 8°N.

the NEC, where the standard deviation is ~0.10 m s^{-1} or 40% of the mean velocity. In two zonal sections, geostrophic velocities vary wildly, attaining maximum standard deviation of the same order as the mean velocity in the Kuroshio and the MC. *Wijffels et al.* [1995] attributed these large variabilities to dynamic height noise amplified by the small station spacing over the shelf break. The dynamic height noise could be due to strong eddies and local effects, especially those associated with the transient upwelling near the coast [*Lukas et al.*, 1991].

It has been shown, however, that geostrophic velocity derived from the mean hydrographic section is in remarkable agreement with the averaged ADCP measurements at 8°N [*Wijffels et al.*, 1995], implying that the dynamic height noise that occurred in the individual sections could be filtered out by averaging. In fact, *Wijffels et al.* [1995] already noted a low variability (<0.10 m s^{-1} or 11% of the mean) of the upper portion of the MC from the ADCP measurements. The situation at 18°N is likely the same. At least, dynamic height shows the smallest variability on the inshore edge of the Kuroshio. The rms of 0/1500 dbar, for example, is 0.10 dynamic meters (dyn. m) in the westernmost bin centered at 122.5°E. The value increases seaward, with a maximum of about 0.20 dyn. m at 125°–126°E. Below the thermocline the LUC and the MUC are evident during all the periods of observation, though considerable variabilities are found among different synoptic sections (Figures 7a and 7b). These appear to suggest that the mean current structure described above (Figures 4a–4c and 6a–6b) should be reasonably representative of the mean conditions.

Individual velocity sections provide ~10 estimates of transport for each flow (Figure 8). The transport fluctuations in the NEC and the Kuroshio are nearly in phase, both showing a seasonal signal with interannual variations superimposed. The coherence of the NEC and the Kuroshio in transport fluctuation has previously been reported [*Yamagata et al.*, 1985; *Qiu and Lukas*, 1996]. For the seasonal variation of the Kuroshio, *Wyrtki* [1961] noted a maximum transport in spring and a minimum transport in fall. Here, indeed, most transport peaks occurred in April–June, and most bottom values took place in September–October. This seasonal signal seems to be submerged by interannual variation associated with the 1986–1987 El Niño and 1988–1989 La Niño events. The transport fluctuation of the MC is found to be dominated by biennial signal, as inferred by *Lukas* [1988] from the sea level data, presumably because of the quasi-biennial surface wind anomalies in the tropics resulting from ocean-atmosphere-land interaction.

It is worth mentioning that the interannual fluctuation of transport associated with ENSO shown in Figure 8 is nearly out of phase with earlier observations. According to *Lukas* [1988] and *Qiu and Joyce* [1992], both the NEC and the MC are stronger than normal during the ENSO events, while the present results indicate that the minimum transport of the current system concurred with the mature phase of the 1986–1987 El Niño and maximum transport took place in the year

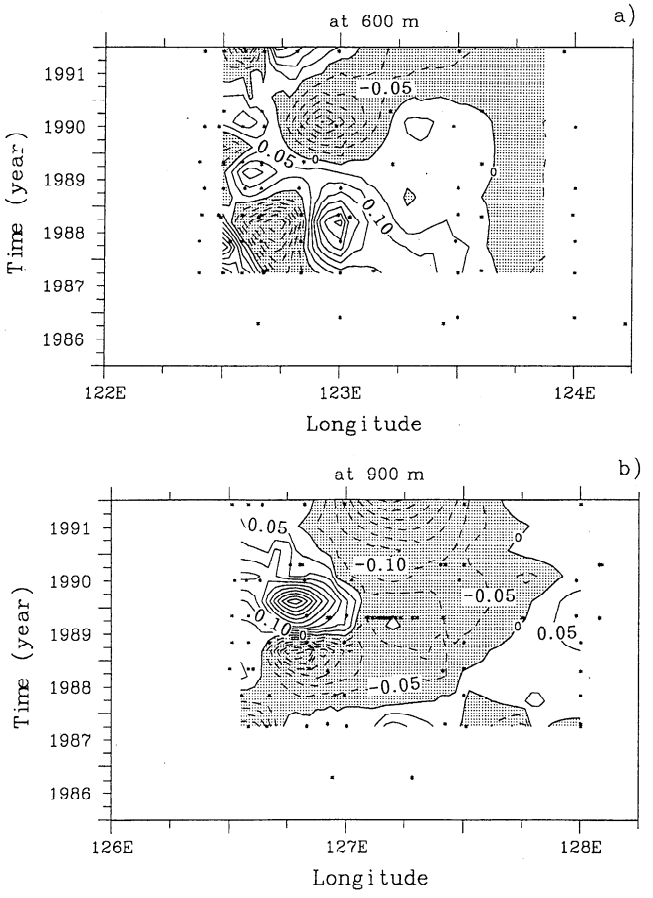

Figure 7. Longitude-time diagram of geostrophic velocities (m s^{-1}) relative to 1500 dbar at (a) 600 dbar east of Luzon and (b) 900 dbar east of Mindanao. The contour intervals are 0.05 m s^{-1}, and positive values are northward for the Kuroshio and southward for the MC.

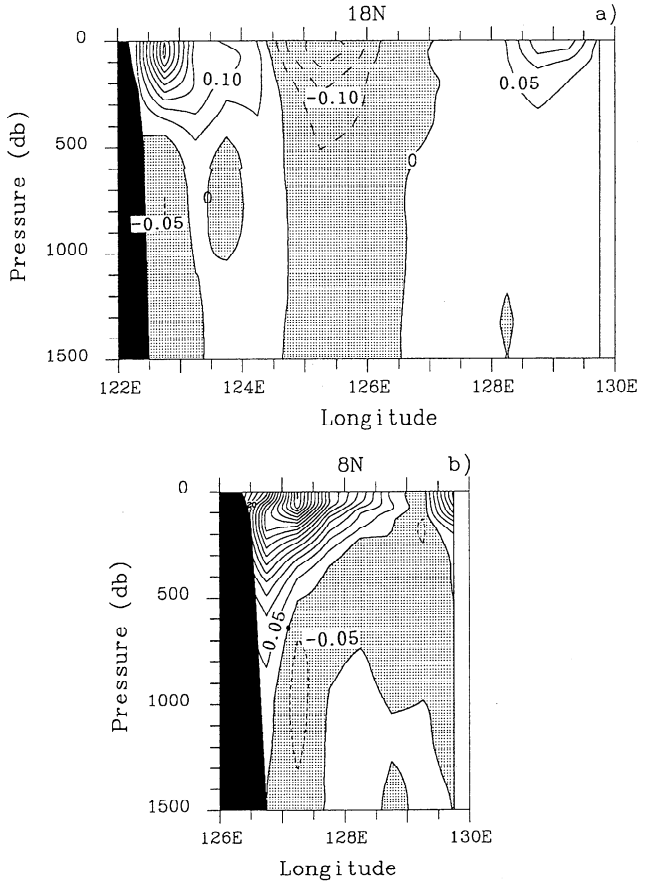

Figure 6. Same as Figure 4, except at (a) 18°N and (b) 8°N with respect to 2000 dbar.

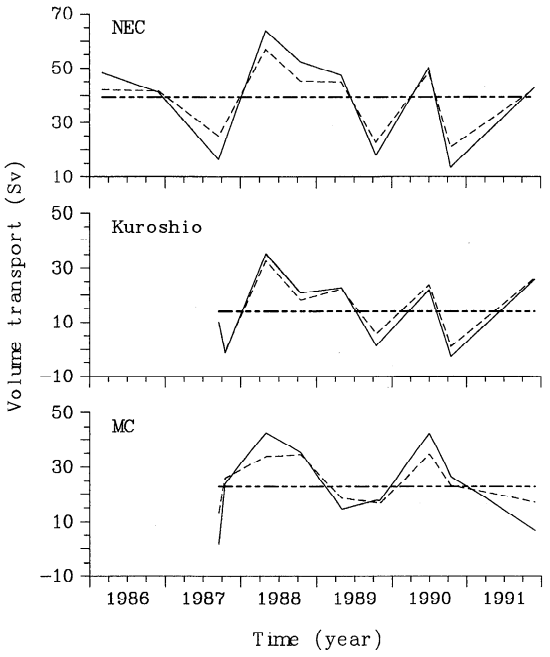

Figure 8. Fluctuations of total (solid lines; 0–1500 db) and upper thermocline (dashed lines; $\sigma_\theta < 26.7$) transport in the NEC, the Kuroshio, and the MC. The dotted-dashed lines represent the average of total transport.

prior to and the year after the event. The reason for the discrepancy is still not clear.

The average of synoptic transports (Table 2) shows similar values to those derived from mean hydrographic sections (Table 1). During the period of observations, upper layer transport varies with an amplitude of ~10 Sv in the current system, accounting for 29% of the mean NEC transport, 70% of the mean Kuroshio transport, and 33% of the mean MC transport. The percentage increases with depth. In the intermediate layer the standard deviation of transport is of the same order as the mean value.

5. Mean Water Property Distribution

The baroclinic structure of the currents is apparent in the mean density distributions (Figures 9a–9c). Isopycnals along 130°E exhibit a shallow pycnocline around the North Equatorial Countercurrent trough, with downward displacement to the north. Within the Kuroshio, upper isopycnals slope up near the coast, while the downward slope of the pycnocline associated with the MC appears to be much broader and rather uniformly distributed along the section. Below the pycnocline, isopycnals reverse their directions in all three sections, indicative of an undercurrent structure.

Two interesting parts of the salinity distribution (Figures 10a–10c) are the following well-defined salinity extremes: the North Pacific Topical Water (NPTW) and the North Pacific Intermediate Water (NPIW). NPTW ($S > 34.9$ practical salinity units (psu)) is seen between 100 and 200 dbar and around $\sigma_\theta = 24.0$. It spreads within the subtropical gyre to ~10°N in the interior ocean (Figure 10a). Along 18°N, the lowest value of salinity (<34.9 psu) at NPTW is found at 127°E, not at the coastal station as expected [*Toole et al.*, 1988]. In fact, at the depths of NPTW, salinity achieves a maximum (>34.95 psu) near the coast, indicative of the direct influence of the Kuroshio. Within the MC, NPTW is seen very close to the coast, consonant with its supply from the North Pacific subtropical gyre [*Nitani*, 1972; *Wijffels et al.*, 1995]. The highest salinity (>34.95 psu), however, resides at about 129°E on this section. This salinity maximum may have originated from the South Pacific via the Halmahera Eddy [*Lukas et al.*, 1991].

The NPIW salinity minimum (<34.4 psu) is confined primarily to north of 12°N along the potential density surfaces around 26.8 kg m ^{3} at 130°E. The water is likely first to come westward from the NEC at around 18°N, depending on the NEC bifurcation latitude, then to turn southward as part of the LUC, and finally to escape to the equatorial region via the MC. At the beginning of the LUC the low-salinity tongue extends westward throughout the section (Figure 10b). According to *Qu et al.* [1997b], ~1 Sv of NPIW (<34.40 psu) is advected to the south by the LUC at 18°N. As NPIW approaches the coast of Mindanao, its salinity minimum hugs the continental slope with a value ~0.15 psu higher than in the LUC because of mixing. Also, as previously observed [*Lukas et al.*, 1991; *Bingham and Lukas*, 1994], NPIW is of lower density (~26.55 kg m^{-3}) at the coast of Mindanao. *Lukas et al.* [1991] suggest that the deep component of NPIW is sheared off by the intrusion of the relatively high salinity Antarctic Intermediate Water (AAIW). Further study is required.

6. Dynamics

6.1. Depth-Integrated Dynamic Height

According to a simple Sverdrop theory [*Godfrey*, 1989], in a semienclosed ocean like the North Pacific the depth-integrated longshore pressure gradient at the western boundary can be determined by basin-scale wind stress alone. For example, let Z and W be two points on the inshore edge of the western boundary current, and let Y and X be the two points at the same latitudes as Z and W on the eastern boundary. The depth-integrated dynamic height (marked as P below) differences between Z and W is given by the integral of the long-path component of wind stress for the path $WXYZ$; that is,

$$P_z - P_w = \int_{WXYZ} \rho_0^{-1} \tau^{(l)}\, dl \qquad (1)$$

Table 2. The Average and Standard Deviation of Synoptic Transports of the NEC, the Kuroshio, and the MC

Relative to 1500 dbar	$\sigma_\theta < 26.7$			$26.7 < \sigma_\theta < 27.1$			27.1 σ_θ-1500 dbar			0–1500 dbar		
	NEC	KC	MC	NEC	KC	MC	NEC	KC	MC	NEC	KC	MC
Mean	39.0	15.0	24.0	4.2	−0.2	3.0	−4.1	−0.9	−3.7	39.4	13.9	23.0
s.d.	11.4	10.7	7.9	3.0	1.2	3.4	2.5	1.3	4.0	16.4	12.3	13.0

Transport and its standard deviation are in Sverdrups. Positive values are westward for the NEC, northward for the Kuroshio Current (KC), and southward for the MC.

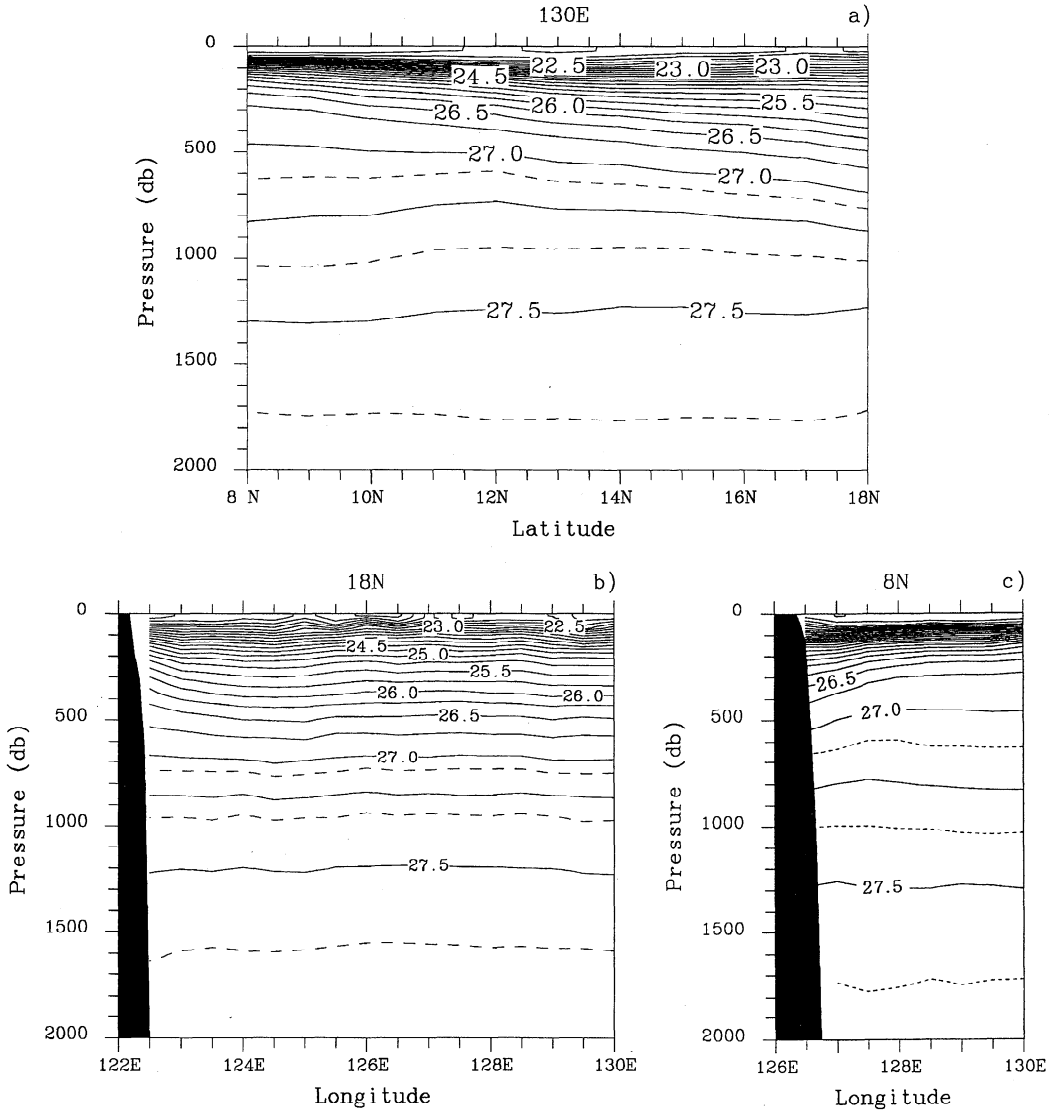

Figure 9. Mean potential density (kg m^{-3}) at (a) 130°E, (b) 18°N, and (c) 8°N. The contour intervals are 0.25 kg m^{-3}.

where ρ_0 is mean water density and $\tau^{(1)}$ is the long-path wind stress component. In the downstream direction of the western boundary currents this difference is typically large compared with that between Y and X on the eastern boundary and provides the pressure head driving the western boundary currents against friction.

Now let us test how well this simple theory fits the western boundary currents near the Philippine coast or, in other words, how much of the longshore pressure gradient in the western boundary currents may be explained by the basin-scale wind stress over the Pacific. The depth-integrated dynamic height P, is first estimated from the observed mean temperature and salinity with respect to 1500 dbar. From 130°E to the shelf edge, P drops by ~56 m^2 at 18°N and rises by ~48 m^2 at 8°N, consonant with the Kuroshio and the MC, respectively. On the inshore edge, P at 13°N is found to be ~8 m^2 higher than at 18°N and ~53 m^2 higher than at 8°N. On the offshore edge, P rises all the way from 8° to 18°N, reflecting the westward directed NEC. The integral of *Hellerman and Rosenstein*'s [1983] annual mean wind stress (1) shows a drop in P of 5 m^2 from 13° to 18°N and a drop of 42 m^2 from 13° to 8°N at the coast, accounting for ~80% of the estimates from the observations. The relatively small difference of P between 13° and 18°N reflects weak northward flow at these latitudes.

On the annual average, local winds are light near the Philippine coast. The longshore integrals of *Hellerman and Rosenstein*'s, [1983] annual mean wind stress are only about -0.2 m^2 from 8° to 13°N and about -1.2 m^2 from 13° to 18°N, smaller by a factor of at least 6 than the observed longshore pressure gradient. This implies that local wind stress may not be important in determining the annual mean western boundary currents in the region, even though they might be effective in inducing seasonal and interannual fluctuations [*Masumoto and Yamagata*, 1991; *Qiu and Lukas*, 1996].

6.2. Depth Dependence of the Longshore Pressure Gradient

Depth dependence of the longshore pressure gradient is indicated in vertical profiles of dynamic height difference between three different latitudes (Figure 11). On the offshore

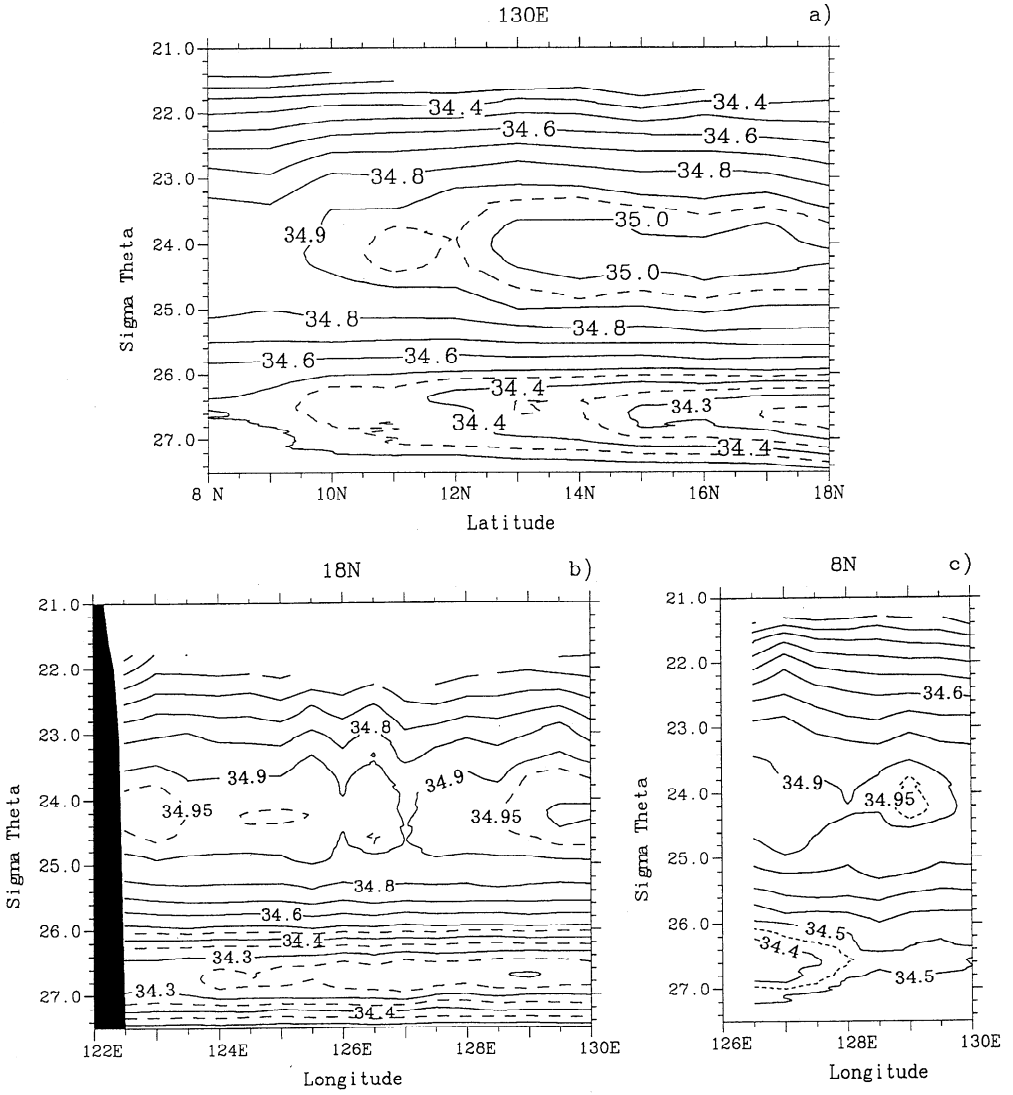

Figure 10. Mean salinity (practical salinity units (psu)) at (a) 130°E, (b) 18°N, and (c) 8°N. The contour intervals are 0.1 psu.

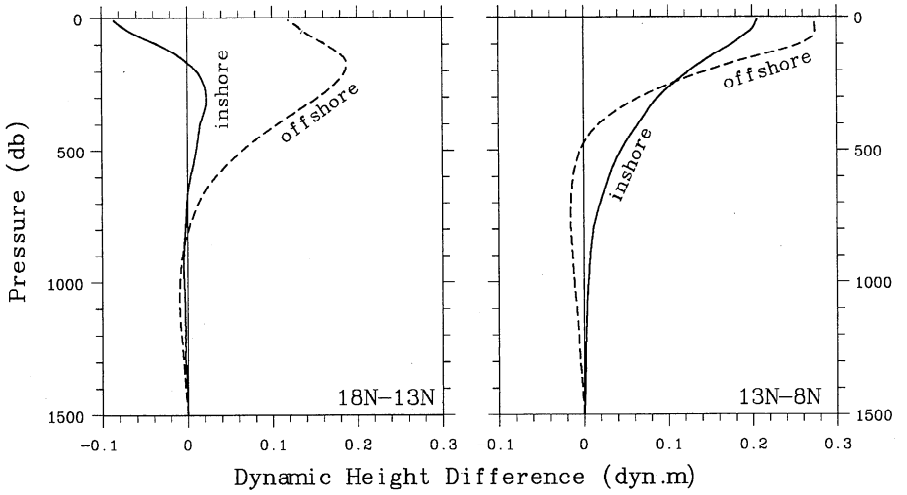

Figure 11. Vertical profiles of mean dynamic height difference (dynamic meters) relative to 1500 dbar between 18° and 13°N and between 13° and 8°N.

edge, dynamic height rises in the upper 500 dbar but drops below that depth from 8° to 13°N, geostrophically, corresponding to a westward flow near the surface and an eastward flow at depth (Figure 4a). A similar profile is seen in the northern region, except that the dynamic height difference changes its signal at a greater (~850 dbar) depth as the NEC spreads to denser waters toward the north.

The vertical profiles on the inshore edge show a considerable difference between the two regions. Dynamic height drops in the downstream direction of the MC at all depths from the surface down to 1500 dbar, providing a pressure head that drives the flow against friction. The pressure gradient in the northern region, however, reverses its direction at ~180 dbar, which, on the meridional average (13°–18°N), is around the boundary between the surface Kuroshio and the subsurface LUC. In general, all these currents flow in the direction of the longshore pressure gradient.

6.3. Forcing Mechanics

Several dynamic aspects of the western boundary currents may be inferred from the picture of the pressure gradient presented in section 6.2. In a sense of linear dynamics the currents are primarily controlled by the following equations:

$$fv = -\frac{1}{\rho}\frac{\partial p}{\partial x} \tag{2}$$

$$-fu = -\frac{1}{\rho}\frac{\partial p}{\partial y} + F_y \tag{3}$$

On the offshore edge the flow is generally geostrophic, and the action of the equatorward directed longshore pressure gradient, $(1/\rho)(\partial p/\partial y)$, is to force a westward flow (NEC). The westward flow is undisturbed from its open ocean value until it runs into the continent, where friction becomes important and breaks the geostrophic constraint. On the inshore edge (defined as the westernmost 0.5°-longitude bin) the longshore pressure gradient can be split up into two parts (3). One creates a cross-shelf flux u via geostrophy, and the second is used to overcome friction F_y.

In the southern region the equatorward directed longshore pressure gradient (Figure 11) causes water to move continuously toward the coast. Because u has to satisfy a condition of zero transport on the shore, water may be accumulated against the coast, and as a result, a cross-shelf pressure gradient, $(1/\rho)(\partial p/\partial x)$, is set up, which eventually generates a southward flow (MC) via geostrophy (2). The downward slope of isopycnals to the west from below the surface (land effects and local winds may be important at the surface) down to at least 1000 dbar in Figure 9c is consistent with the near-shore convergence, allowing the MC to penetrate to a greater depth than the NEC in the southern region (Figures 4a and 4c). The rest of the longshore pressure gradient, that is, the imbalance between $(1/\rho)(\partial p/\partial y)$ and fu, provides a necessary condition for the MC to go against friction.

Within the Kuroshio the surface NEC is not likely to flow directly toward the coast; otherwise, water accumulation on the inshore edge would produce an equatorward flow in the same way as in the MC. Instead, water near the coast may be sucked from the subsurface and carried offshore as a result of the poleward directed longshore pressure gradient in the surface layer (Figure 11). In a general case of poleward western boundary currents this has previously been suggested by *Godfrey* [1973a], who also noticed that the existence of upwelling in the East Australian Current may sometimes be traced by surface nutrient distribution [*Godfrey*, 1973b]. The divergence on the inshore edge of the Kuroshio seems to be identical to the upward slope of isopycnals to the west from the surface to ~700 dbar (Figure 9b), which may explain why the Kuroshio is confined only to the upper 500 dbar (Figure 4b) despite the fact that the NEC extends to as deep as 800 dbar east of Luzon (Figure 4a).

7. Summary

With repeated hydrographic sections we have shown a relatively reliable picture of the current structure and transport in the NEC-Kuroshio-MC system near the Philippine coast. Most of the present results are based on geostrophic calculation by assuming a 1500-dbar reference level (the deepest common depth of the observations). However, it has been indicated that both the current structure and transport are insensitive to vertical displacements of the reference level within the depth range between 1500 and 2500 dbar. Examination of potential density vertical shear suggests that the best choice for the reference level is ~2000 dbar. With this depth of no motion, transport estimates achieve a mass balance better than 2 Sv in a region enclosed by stations.

The averaged current structure from individual velocity sections (relative to 1500 dbar) shows surprisingly good agreement with that derived from mean hydrographic sections. A prominent feature of the averaged current structure is the countercurrent structure below the surface flow, that is, the eastward flow underlying the NEC, the southward flowing LUC, and the northward directed MUC. The main part of the LUC appears to be closely related to the northward shift of the NEC with increasing depth. From the highly smoothed climatological data it is inferred that the NEC bifurcates at around 18°N at 500 m, while results from numerical models [e.g., *Kagimoto and Yamagata*, 1997] indicate that the bifurcation could occur as far north as 20°N in the intermediate layer.

The MUC was observed in all synoptic sections, with a high-speed (>0.08 m s^{-1}) core at about 900 dbar and 75–100 km offshore on the average. In this sense, the MUC is not likely to be merely a transient phenomenon. It should be a permanent feature. However, mean water mass distribution does not show any significant property core in the narrow MUC, though a relatively high oxygen level characteristic of AAIW was indeed found in a broad region off Mindanao [*Wijffels et al.*, 1995]. It is possible that the MUC is mainly a component of local recirculation associated with the Halmahera Eddy. Further study is required.

Geostrophic flow exhibits extremely large variabilities at the western boundary, supporting *Lukas et al.*'s [1991] hypothesis that geostrophic estimate of velocity may be substantially aliased because of strong eddies and internal tides in the region. There are indications that variability of the MC in directly measured velocity is much less than that in geostrophic flow, despite remarkable agreement between the mean sections [*Wijffels et al.*, 1995]. This seems to mean that the dynamic height noise associated with high-frequency activities could be largely filtered out by averaging, so the mean velocity structure and transport described in this study should be reasonably representative of the mean conditions in the NEC-Kuroshio-MC system.

The present data set also allows an estimate of transport

fluctuations in a consistent way for the NEC-Kuroshio-MC system. The rms of transport in the upper thermocline is found to be ~10 Sv. It is interesting that although the individual velocity sections may be affected strongly by eddies and internal tides, the transport fluctuations demonstrate many features similar to earlier observations. The NEC and the Kuroshio vary in transport almost in the same phase, with a seasonal signal superimposed with interannual variations, and the MC transport is dominated by a biennial oscillation. Outstanding questions are why and how the maximum transport of the current system does not occur in the mature phase of ENSO, as previously suggested, but takes place prior to and after the event.

The depth-integrated dynamic height distribution is found to be consistent with the simple Sverdrop theory, reflecting the dominant influence of the basin-scale wind stress on the current system. With depth dependence, longshore pressure gradient changes its direction at nearly the same depth as the current changes its direction. From a point of view of linear dynamics several aspects of the current system are examined. Among them, we suggest a divergence of mass on the inshore edge of the Kuroshio and a convergence of mass on the inshore edge of the MC. The nonlinear dynamics (e.g., the advective terms in the momentum equations) might be required to adequately describe the western boundary currents, and it will certainly make things more complicated. Much work could be done with the emergence of high-resolution ocean general circulation models.

Acknowledgments. This study benefited from discussions with Gary Meyers, Stuart Godfrey, Dunxin Hu, and Roger Lukas. We thank Nelson Hogg, Peter Hacker, and two anonymous reviewers for their valuable comments and suggestions on the earlier manuscript. The CAS data were kindly provided by the Institute of Oceanology, Chinese Academy of Sciences, and the PRC-US data were provided by the State Oceanic Administration Data Center of China.

References

Bingham, F. M., and R. Lukas, The southward intrusion of North Pacific Intermediate Water along the Mindanao coast, *J. Phys. Oceanogr.*, *24*, 141–154, 1994.

Fine, J. S., R. Lukas, F. M. Bingham, M. J. Warner, and R. H. Gammon, The western equatorial Pacific is a water mass crossroads, *J. Geophys. Res.*, *99*, 25,063–25,080, 1994.

Godfrey, J. S., On the dynamics of the western boundary current in Bryan and Cox's (1968) numerical model ocean, *Deep Sea Res. Oceanogr. Abstr.*, *20*, 1043–1058, 1973a.

Godfrey, J. S., Comparison of the East Australian Current with the western boundary flow in Bryan and Cox's (1968) numerical model ocean, *Deep Sea Res. Oceanogr. Abstr.*, *20*, 1059–1076, 1973b.

Godfrey, J. S., A Sverdrup model of the depth-integrated flow for the world ocean allowing for island circulations, *Geophys. Astrophys. Fluid Dyn.*, *45*, 89–112, 1989.

Gordon, A. L., Interocean exchange of thermocline water, *J. Geophys. Res.*, *91*, 5037–5046, 1986.

Gouriou, Y., and J. Toole, Mean circulation of the upper layers of the western equatorial Pacific Ocean, *J. Geophys. Res.*, *98*, 22,495–22,520, 1993.

Guan, B., Major features of warm and cold eddies south of the Nansei Islands, *Chin. J. Oceanol. Limnol.*, *1*, 248–257, 1983.

Hellerman, S., and M. Rosenstein, Normal monthly wind stress over the world ocean with error estimates, *J. Phys. Oceanogr.*, *13*, 1093–1104, 1983.

Hu, D., M. Cui, T. Qu, and Y. Li, A subsurface northward current off Mindanao identified by dynamic calculation, in *Oceanography of Asian Marginal Seas, Elsevier Oceanogr. Ser.*, vol. 54, edited by K. Takanao, pp. 359–365, Elsevier, New York, 1991.

Kagimoto, T., and T. Yamagata, Seasonal transport variations of the Kuroshio: An OGCM simulation, *J. Phys. Oceanogr.*, *27*, 403–418, 1997.

Levitus, S., Climatological atlas of the world oceans, *NOAA Prof. Pap. 13*, U.S. Gov. Print. Off., Washington, D. C., 1982.

Lukas, R., Interannual fluctuations of the Mindanao Current inferred from sea level, *J. Geophys. Res.*, *93*, 6744–6748, 1988.

Lukas, R., E. Firing, P. Hacker, P. L. Richardson, C. A. Collins, R. Fine, and R. Gammon, Observations of the Mindanao current during the Western Equatorial Pacific Ocean Circulation Study, *J. Geophys. Res.*, *96*, 7089–7104, 1991.

Lukas, R., T. Yamagata, and J. P. McCreary, Pacific low-latitude western boundary currents and the Indonesian throughflow, *J. Geophys. Res.*, *101*, 12,209–12,216, 1996.

Masumoto, Y., and T. Yamagata, Response of the western tropical Pacific to the Asian winter monsoon: The generation of the Mindanao Dome, *J. Phys. Oceanogr.*, *21*, 1386–1398, 1991.

McCreary, J. P., and P. Lu, Interaction between the subtropical and equatorial ocean circulations: The Subtropical Cell, *J. Phys. Oceanogr.*, *24*, 466–497, 1994.

Meyers, G., R. J. Bailey, and A. P. Worby, Geostrophic transport of Indonesian throughflow, *Deep Sea Res., Part I*, *42*, 1163–1174, 1995.

Nitani, H., Beginning of the Kuroshio, in *Kuroshio: Physical Aspects of the Japan Current*, edited by H. Stommel and K. Yoshida, pp. 129–163, Univ. of Washington Press, Seattle, Wash., 1972.

Qiu, B., and T. Joyce, Interannual variability in the mid- and low-latitude western North Pacific, *J. Phys. Oceanogr.*, *22*, 1062–1079, 1992.

Qiu, B., and R. Lukas, Seasonal and interannual variability of the North Equatorial Current, the Mindanao Current, and the Kuroshio along the Pacific western boundary, *J. Geophys. Res.*, *101*, 12,315–12,330, 1996.

Qu, T., G. Meyers, J. S. Godfrey, and D. Hu, Upper ocean dynamics and its role in maintaining the annual mean western Pacific warm pool in a global GCM, *Int. J. Climatol.*, *17*, 711–724, 1997a.

Qu, T., T. Kagimoto, and T. Yamagata, A subsurface countercurrent along the east coast of Luzon, *Deep Sea Res., Part I*, *44*, 413–423, 1997b.

Reid, J. L., and R. S. Arthur, Interpretation of maps of geopotential anomaly for the deep Pacific Ocean, *J. Mar. Res.*, *33*, suppl., 37–52, 1975.

Toole, J. M., E. Zou, and R. C. Millard, On the circulation of the upper waters in the western equatorial Pacific Ocean, *Deep Sea Res., Part A*, *35*, 1451–1482, 1988.

Toole, J. M., R. C. Millard, Z. Wang, and S. Pu, Observations of the Pacific North Equatorial Current bifurcation at the Philippine coast, *J. Phys. Oceanogr.*, *20*, 307–318, 1990.

Wijffels, S., E. Firing, and J. Toole, The mean structure and variability of the Mindanao Current at 8°N, *J. Geophys. Res.*, *100*, 18,421–18,435, 1995.

Wyrtki, K., Physical oceanography of the southeast Asian waters, *Naga Rep.*, *2*, 195 pp., Scripps Inst. of Oceanogr., LaJolla, Calif., 1961.

Yamagata, T., Y. Shibao, and S. Umatani, Interannual variability of the Kuroshio extension and its relation to the Southern Oscillation/El Nino, *J. Oceanogr. Soc. Jpn.*, *41*, 274–281, 1985.

H. Mitsudera, International Pacific Research Center, SOEST, University of Hawaii, 2525 Correa Road, Honolulu, HI. (e-mail: humiom@soest.hawaii.edu)

T. Qu, Ocean Research Department, Japan Marine Science and Technology Center, 2-15 Natsushima, Yokosuka 237, Japan. (e-mail: tangdong@jamstec.go.jp)

T. Yamagata, Department of Earth and Planetary Physics, Tokyo University, Tokyo 113, Japan. (e-mail: yamagata@geoph.s.u-tokyo.ac.jp)

(Received January 24, 1997; revised October 20, 1997; accepted December 1, 1997.)